Toward Free-Living Walking Speed Estimation Using Gaussian Process-based Regression with On-Body Accelerometers and Gyroscopes

Harshvardhan Vathsangam†, Adar Emken*, Donna Spruijt-Metz*, Gaurav S. Sukhatme†
(vathsang | emken | dmetz | gaurav) @ usc.edu

†Robotic Embedded Systems Laboratory
Department of Computer Science
University of Southern California

*Spruijt-Metz Lab
Department of Preventive Medicine
University of Southern California

***Abstract*—Walking speed is an important determinant of energy expenditure. We present the use of Gaussian Process-based Regression (GPR), a non-linear, non-parametric regression framework to estimate walking speed using data obtained from a single on-body sensor worn on the right hip. We compare the performance of GPR with Bayesian Linear Regression (BLR) and Least Squares Regression (LSR) in estimating treadmill walking speeds. We also examine whether using gyroscopes to augment accelerometry data can improve prediction accuracy. GPR shows a lower average RMS prediction error when compared to BLR and LSR across all subjects. Per subject, GPR has significantly lower RMS prediction error than LSR and BLR ($p<0.05$) with increasing training data. The addition of tri-axial gyroscopes as inputs reduces RMS prediction error ($p<0.05$ per subject) when compared to using only acclerometers. We also study the effect of using treadmill walking data to predict overground walking speeds and that of combining data from more than one person to predict overground walking speed. A strong linear correlation exists ($r_{X,Y} = .8861$) between overground walking speeds predicted from treadmill data and ground truth walking speed measured. Combining treadmill data from multiple subjects with similar height characteristics improved the prediction capability of GPR for overground walking speeds as measured by correllation between ground truth and GP-predicted values ($r_{X,Y} = .8204$ with combined data).**

Keywords: Gaussian processes, Accelerometers, Gyroscopes, Walking speed estimation

I. Introduction

Nearly half the United States population (45%) is expected to be obese by 2020, decreasing life expectancy and quality of life significantly [1]. It is believed that weight gain could be prevented by achieving small changes in behavior, such as 15 minutes per day of walking [2]. Walking is the most common type of activity among people who are physically active [3]and a critical component in energy expenditure[4]. In the face of the current obesity epidemic, findings suggest that encouraging walking habits in the general population could be effective in preventing and reducing obesity [5]. Therefore, accurate detection of walking speed could be a valuable tool in enhancing public health.

Over the past decade, there has been considerable research directed towards the detection and classification of physical activity patterns from body mounted inertial sensors [6]. Typical inertial sensors contain an accelerometer with two or more gyroscopes to provide kinematic information. Accelerometers and gyroscopes have been combined to determine orientation of human body segments [7] and to track the center of mass of trunk movement [8]. These studies make the implicit assumption that an inertial sensor provides motion information of the segment to which it is attached. We adopt the same assumption and rely on data-driven pattern recognition techniques to derive estimates of motion from inertial data. The use of pattern recognition techniques to determine parameters of energy expenditure is not new [9], [10]. Accelerometer outputs have been correlated to treadmill and overground walking speeds using linear and quadratic regression models [11]. These parametric models need to adequately represent the structure of the modeled data to be accurate. They also require a lot of clean, complete, and uncorrelated data to be properly validated. In this context, we introduce the application of Gaussian Process based Regression (GPR), a non-parametric data driven regression technique in estimating walking speeds. In non-parametric methods such as GPR, the model structure is not specified a priori but is instead determined from data. Accelerometers have also been used with neural networks in detecting speed and incline of outdoor walking[12]. Choosing the optimal number of hidden units (and hence the complexity of the hidden layer) in conventional neural networks relies on heuristics or cross-validation. Also, a large number of parameters to train for means that neural networks are prone to overfitting. By contrast, since GPR is data-driven, model complexity is derived from the data itself. GPR also uses a probabilistic approach to model prediction uncertainty thus eliminating the need for cross-validation.

The human body can be modeled as a series of interconnected rigid objects, each of which can be rotated or translated relative to its neighbors in free space [13]. The assumption behind using accelerometry for physical activity monitoring is that data from an accelerometer represents body movement [14]. Rigid body movement however consists of both accelerations and rotations. Therefore, to track a rigid body one should track both translations and rotations. However, rotational data cannot be completely separated from translational data from a single triaxial accelerometer [15]. Thus, there is merit in tracking rotational rates separately. We use this idea to examine whether addition of gyroscopes can enhance walking speed estimation.

Walking speed estimation algorithms lack a consistent, scalable ground truth on which to base training. One approach is to use ground truth obtained from a treadmill to estimate overground walking speed. Studies have explored whether activity parameters derived from treadmill walking could be used in overground walking [16]. We build on these studies with an experimental evaluation of using data from treadmill walking to predict speeds in overground walking using inertial sensing.

In this paper, we address the problem of estimating walking speed using on-body inertial sensing using GPR. We use an

PERVASIVEHEALTH 2010, March 22-25, Munchen, Germany

DOI 10.4108/ICST.PERVASIVEHEALTH2010.8786

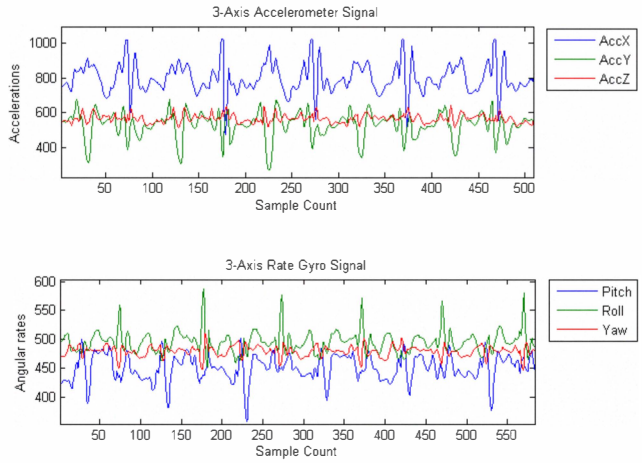

(a) An example of periodic signals obtained from the right hip of a single subject while walking at a constant speed of 2.5 mph.

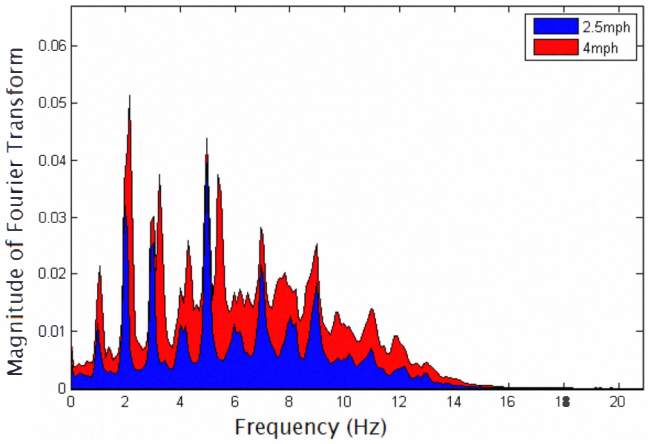

(b) The Fourier transforms of the accelerometer stream from a single subject on the X-axis for steady state walking at 2.5 mph and 4 mph. Definite peaks that are characteristic of the walking speed suggest speed estimation by monitoring the frequency spectrum

Figure 1: Periodicity in walking signals obtained from inertial sensor data from one subject on the illiac crest of the right hip

inertial sensor that combines data from a tri-axial accelerometer and a triaxial gyroscope and show how the frequency characteristics of these signals are related to speed of walk in Sec. II. We show how one can take advantage of functional maps between periodicities and speeds to train a Gaussian Process based Regression (GPR) model in Sec. III. To our knowledge, GPR with inertial sensing has not been used for walking speed estimation. We describe two experimental studies in Sec. IV. The first is a comparative analysis of GPR with well-known regression techniques such as Least Squares Regression (LSR) and Bayesian Linear Regression (BLR). We also study the effect of varying window size and addition of gyroscopes. The results of this study are in Sec. V-A. The second study describes the effects of combining treadmill and overground walking data on predicting overground walking speeds. The results of this study are in Sec. V-B1.
Our results demonstrated that GPR had a lower average RMS prediction error when compared to BLR and LSR across all subjects and a significantly lower RMS prediction error ($p<0.05$) on one subject. A strong linear correlation existed ($r_{X,Y} = .8861$) between overground walking speeds predicted from treadmill data and ground truth walking speed measured. Combining treadmill data from multiple subjects with similar height characteristics improved the overground speed prediction capability of GPR.

II. A Frequency-Based Interpretation Of Walking

A. Periodicity in Walking

Steady state walking is cyclic. There is a wealth of literature in examining the gait cycles in walking and the associated periodic limb movements [17], [18]. Our approach involves capturing this inherent periodicity from a single inertial sensor worn above the illiac crest on the right hip. Fig. 1a shows a typical plot of the signals received while walking at a constant speed of 2.5 mph. Movement data are captured in the form of six time series using a tri-axial accelerometer and tri-axial rate gyroscope. These signals correspond directly to the accelerations and rotational rates of the hip as felt by the sensor in its local frame of reference.

We examine the periodicity of this signal by computing its Fourier transform. The blue area of Fig.1b is the Fourier transform of the accelerometer signal as measured on the X-axis. The transform consists of peaks at definite frequencies. The peaks occur at the same frequencies for the other sensor streams (in all 3 axes) as well. Furthermore, the location of these peaks is a function of walking speed. In the same figure, the red area is the Fourier transform of the X-axis acceleration signal while walking at 4 mph. The peaks are shifted to the right indicating higher frequency components. This is because walking at higher speeds takes a smaller time period per gait cycle implying higher frequency components. This suggests that one can track walking speeds using the frequency spectrum as a representation of periodicity.

B. A Visualization of Signal Periodicity with Changing Walking Speed

To visualize how walking speeds evolve with changes in the frequency spectra of movement signals, and to explore whether these features can be mapped to their corresponding speeds, we performed a Principal Component Analysis (PCA). Fig. 2 illustrates a 3-dimensional visualization of the first three components of the frequency spectra for a range of walking speeds from 2.5 mph to 4 mph increased in steps of 0.1 mph for five minutes per speed. Ground truth for these speeds was recorded on a treadmill. Data recording and feature extraction procedures are outlined in Sec. IV. Variance preserved in the first three components is 76%. The visualization shows that there is indeed a continuous evolution of feature vectors with changing speed. We thus formulate the hypothesis that one can estimate walking speed by tracking these features and aim to find this estimation map.

C. Mapping Periodicities to Walking Speeds

We use Gaussian Process based Regression (GPR) to find the correspondence between feature vectors and the speed of walking. GPR was chosen because it represents a data driven regression method. The utility of GPR stems from its ability to define a probabilistic model over data, mitigating the effects of overfitting and avoiding cross-validation. GPR is described

Digital Object Identifier: 10.4108/ICST.PERVASIVEHEALTH2010.8786
http://dx.doi.org/10.4108/ICST.PERVASIVEHEALTH2010.8786

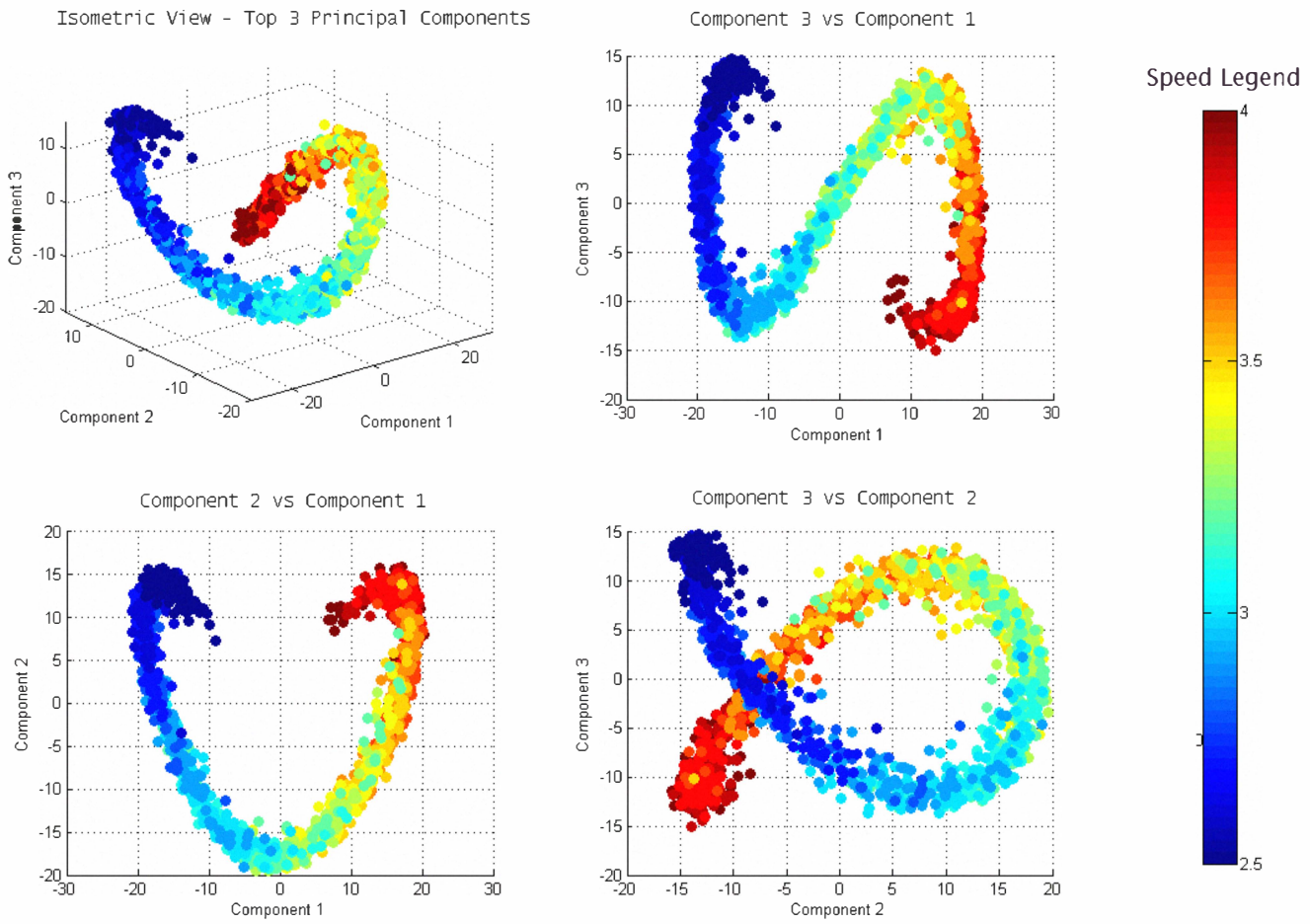

Figure 2: A PCA Based Visualization of Walking Speeds: The color bar indicates ground truth speed. Each figure shows an evolution of the top 3 principal components of the Fourier transforms of windowed sensor signals. A clear evolution of features with increasing speed is seen. This shows that speed can be tracked by observing the periodicity in walking signals using Fourier transforms.

in terms of kernels, avoiding the explicit introduction of a feature space allowing us to use feature spaces of infinite dimensionality thus allowing non-linear mapping.

We compare our approach to Least Squares Regression (LSR) and Bayesian Linear Regression (BLR). LSR offers a baseline performance comparison with GPR. BLR allows comparison of GPR to a probabilistic parametric model. BLR was chosen to avoid the issues of cross validation and over fitting (BLR also incorporates a probabilistic framework). We restrict our experiments to straight line walking to isolate the effect of speed on inertial sensor data.

III. Gaussian Process Background

A. Definition

A Gaussian Process (GP)[19], [20] is defined as a probability distribution over functions $f(x_1), f(x_2), \ldots f(x_N)$ evaluated at points $x_1, x_2, \ldots x_N$ such that any finite subset of the functions $\{f(x_i)\}_{i=1}^{N}$ has a joint multivariate Gaussian distribution. Consequently, for a given set of points $\mathbf{x}=[x_1\, x_2\, \ldots x_N]^T$, we have a corresponding vector $\mathcal{F}_x = [f(x_1)\, f(x_2)\, \ldots f(x_N)]^T$ that belongs to a multivariate Gaussian distribution,

$$\mathcal{F}_x \quad \sim \quad \mathcal{N}\{\mu(\mathbf{x}), k(\mathbf{x}, \mathbf{x})\} \tag{1}$$

where $\mu(\mathbf{x})$ is the prior mean function $[\mu(x_1)\, \mu(x_2) \ldots \mu(x_N)]$ and k is the *kernel* function. The kernel function for two points x_i and x_j, given by $k(x_i, x_j)$, returns the covariance between the corresponding $\mathcal{F}_x$ variables $f(x_i)$ and $f(x_j)$. To completely specify a GP, it is enough to specify the parameters $\mu(\mathbf{x})$ and $k(\mathbf{x}, \mathbf{x}')$. Each $f(x_i)$ is marginally Gaussian, with mean $\mu(x_i)$ and variance $k(x_i, x_i)$.

In our work, the input data space $\{x_i\}_{i=1}^{N}$ is the Fourier transform of the windowed time series of all six sensor streams. The output functions $\{f(x_i)\}_{i=1}^{N}$ are the ground truth speeds. These are measured off-body using ground truth from a treadmill or a distance wheel as outlined in Sec. IV.

B. Gaussian Process Regression

Training a GPR model is equivalent to modeling a joint distribution over the speed mapping functions $\{f(x_i)\}_{i=1}^{N}$ and using this model to map an unknown data point to its corresponding speed. Consider a target quantity t_{x_n} that needs to be predicted for a given x_n. In general, t_{x_n} need not be a linear map nor observable directly. We assume that our mapping function $f(x_n)$ is the required t_{x_n} with an additive noise component, i.e., $t_{x_n} = f(x_n) + \epsilon$, where $\epsilon \sim \mathcal{N}(0, \sigma_\epsilon^2)$. This ensures that the expected value of t_{x_n}, $E[t_{x_n}] = f(x_n)$.

It follows that $p(t_{x_n}|f(x_n)) = \mathcal{N}(t_{x_n}|f(x_n), \sigma_\epsilon^2)$ or in general, $p(\mathbf{t}|f(\mathbf{x})) = \mathcal{N}(\mathbf{t}|f(\mathbf{x}), \sigma_\epsilon^2 I_\mathbf{N})$, where N is the size of the data space. Also, we know that $\mathcal{F}_x \sim \mathcal{N}\{\mu(\mathbf{x}), k(\mathbf{x}, \mathbf{x})\}$. In the absence of prior knowledge about $\mu(\mathbf{x})$, we assume $\mu(\mathbf{x})$=$\mathbf{0}$.

Digital Object Identifier: 10.4108/ICST.PERVASIVEHEALTH2010.8786
http://dx.doi.org/10.4108/ICST.PERVASIVEHEALTH2010.8786

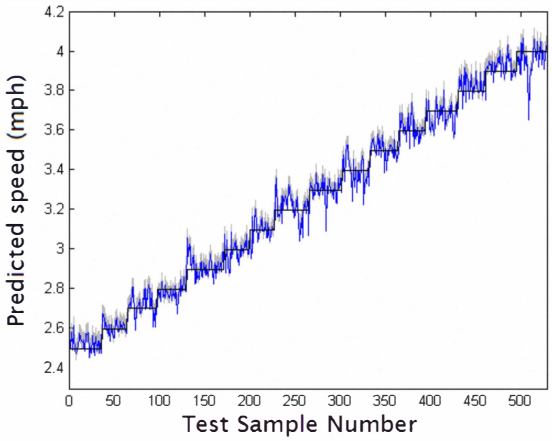

Figure 3: An example of predicting walking speeds using GPR on one subject. The black line indicates ground truth from treadmill data, the blue line indicates the predicted value and the grey background is one standard deviation interval. Modelling uncertainty is a key-property of GPR

It can be shown that,

$$p(\mathbf{t}) = \mathcal{N}(\mathbf{t}|\mathbf{0}, \mathbf{C}_N), \tag{2}$$

where $C(x_i, x_j) = k(x_i, x_j) + \sigma_\epsilon^2 \delta_{ij} \forall i, j = 1, 2, \ldots N$. For a new point $\tilde{x}$, there exists a corresponding target quantity $t_{\tilde{x}}$. Since $t_{\tilde{x}}$ also belongs to the same GP, it can be appended to the original target set to obtain a larger set $\mathbf{t}_{N+1}$, such that,

$$p(\mathbf{t}_{N+1}) = \mathcal{N}(\mathbf{t}_{N+1}|\mathbf{0}, \mathbf{C}_{N+1}) \tag{3}$$

Because this joint distribution is Gaussian by definition, we have,

$$\mathbf{C}_{N+1} = \begin{pmatrix} \mathbf{C}_N & \mathbf{k} \\ \mathbf{k}^T & c \end{pmatrix} \tag{4}$$

where $\mathbf{k}$ has elements $k(x_n, x_{N+1})$ for $n = 1, \ldots, N$ and $c = k(x_{N+1}, x_{N+1}) + \sigma_\epsilon^2$. From this, we evaluate the conditional distribution, $p(t_{N+1}|\mathbf{t})$, which is a Gaussian distribution with,

$$m(x_{N+1}) = \mathbf{k}^T \mathbf{C}_N^{-1} \mathbf{t} \tag{5}$$

$$\sigma^2(x_{N+1}) = c - \mathbf{k}^T \mathbf{C}_N^{-1} \mathbf{k} \tag{6}$$

Thus estimating a target speed from training data amounts to evaluating $\mathbf{C}_N$, $\mathbf{k}$ and $\mathbf{c}$ and using these values shown in Eqs. 5 and 6.

C. Choosing an Appropriate Kernel Function

To reflect that feature vectors with small interpoint Euclidian distance are more likely to output the same walking velocities while capturing the common periodicity represented by feature vectors due to an underlying periodicity in walking we choose the radial basis function kernel. The complete kernel with noise modelling is therefore,

$$k(x_i, x_j) = \sigma_f^2 . e^{-\frac{1}{2}(x_i - x_j)^T S (x_i - x_j)} + \sigma_\epsilon^2 \delta_{ij} \tag{7}$$

D. An Example of GPR in Estimate Walking Speeds

Fig. 3 illustrates an example of a particular training-testing instance of GPR on a single subject. The grey background indicates the confidence interval for the prediction up to one standard deviation. The usage of confidence intervals illustrates the merit of using a probabilistic approach. Using a probabilistic approach means that one need not rely on cross-validation or heuristics to determine model complexity. It also means that one can evaluate the confidence of a prediction when making decisions based on that prediction.

IV. Experimental Study

We present a comparative experimental study to evaluate the utility of GPR applied to walking speed estimation from inertial sensor data. The study is in two parts. In order to test the algorithm with a readily available ground truth and examine the tradeoffs in tuning parameters, we performed a series of tests on a treadmill. The results of this study are described in Sec. V-A. Second, we studied how GPR-based speed estimation is affected by using training data from treadmill walking alone and from combinations of treadmill and overground walking. These results are described in Sec. V-B.

A. Hardware

A modified version of the Sparkfun 6DoF Inertial Measurement Unit (IMU) [21] was used to collect motion information. Data were sampled at 100 Hz. The unit uses Bluetooth to transmit data to either a nearby PC or mobile phone. The use of sensors in all three axes allows us to capture periodicity in all three planes – sagittal, frontal and transverse.

B. Test Population and Experimental Methods

Eight healthy adults (four men, four women) of varying heights, weights and ages (subjects 1-8) walked at 7 pre-determined speeds (2.5 mph, 2.8 mph, 3.0 mph, 3.3 mph, 3.5 mph, 3.8 mph, 4.0 mph), or until breaking into a run. The duration of walking at each speed was 5 minutes. Table I describes the study subjects. All subjects wore a single inertial sensor above the illiac crest on the right hip as shown in Fig. 4b. Subjects were asked to wear the belt tightly to prevent any slippage. The treadmill used for the experiments was the research quality NordicTrack A2550 PRO. Subjects were deliberately chosen to represent a cross-section of heights, ages, Body Mass Indices (BMI) and both genders to demonstrate the utility of GPR across a diverse population. Ground truth for treadmill walking was the displayed treadmill speed.

Attribute	Mean	SD	Max Value	Min Value
Age (yrs)	33	10	48	23
Height (m)	1.75	0.12	1.85	1.58
BMI	26.4	5.3	34.5	22.0

Table I: Statistics of Test Population

Additionally, data of a finer granularity were obtained from a different healthy adult (Subject 9, Age 23, Height 1.82m, BMI 21) who walked at 16 pre-determined speeds from 2.5 to 4.0 mph for 10 min per speed in intervals of 0.1 mph. For each recording of overground walking, Subject 9, wearing an inertial sensor on the right hip walked for a period of 11 seconds in a straight line on a flat, hard surface indoors. The distance moved during the recording (in metres) was measured using a distance wheel, as shown in Fig. 4c. A set of 80 such recordings were made.

C. Feature Computation

Each signal was passed through a bandpass filter with 3dB cutoff between 0.1 Hz and 20 Hz. These cut-off frequencies were chosen keeping in mind that everyday activities fall in the frequency range of 0-10 Hz. The feature vector is computed

Digital Object Identifier: 10.4108/ICST.PERVASIVEHEALTH2010.8786
http://dx.doi.org/10.4108/ICST.PERVASIVEHEALTH2010.8786

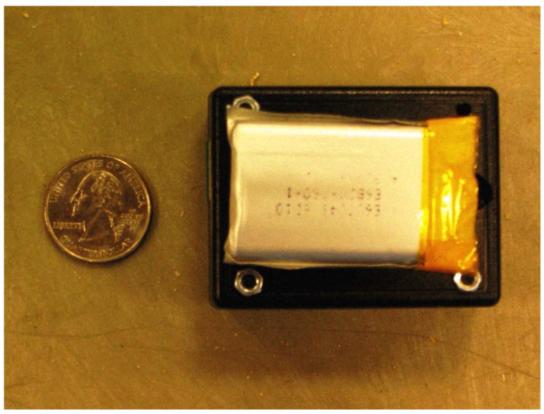

(a) Modified Sparkfun 6DoF inertial sensor used, (Dimensions: 3.6" x 2.4" x 1")

(b) Example mount of the inertial Sensor on the right hip

(c) Overground walking data ground truth collection using a distance wheel

Figure 4: Hardware Setup shows the inertial sensor, its mounting on the hip and a typical data collection in free walking situation

on sliding windows with 50% overlap by finding their N-point FFT. The optimum window size was chosen in hindsight from experimental results (Sec.V-A3) as 1024 samples per window over 512 samples. From experimental results it was shown that the increased frequency resolution of the 1024 point FFT results in lower average RMS error. The complete feature vector consists of the Fourier transforms of the respective window instants for each sensor stream.

V. Results

We describe the experimental results in two sections. Sec. V-A shows results from studies conducted on treadmill data alone. Sec. V-B describes results predicting overground walking speed using models based on treadmill data.

A. Predicting Treadmill Walking Speed

1) Testing Procedure: For treadmill walking, a fraction of recorded data was randomly sampled and partitioned into training data for each subject. The remaining fraction constituted test data. For each algorithm, five separate training runs were executed for each subject. After each training phase, the algorithm was tested on the remaining data points to predict the walking speeds. RMS error was calculated for each instance of test data and the results were averaged over the five runs to combat sample bias. This constitutes a measure of performance of each algorithm per subject. These results were then averaged over all subjects to provide a complete comparative picture of the performance of the three algorithms.

2) Relative Performance of Algorithms: Fig. 5 summarizes the results of increasing the relative size of the training data on the mean and variance of average RMS prediction error across subjects. This provided insight into how much of the dataset should be partitioned and used for training, beyond which reduction in RMS error is minimal. Average RMS error reduced with increase in training data size. Beyond 50% training data, additional training data yielded small reductions in RMS error. For small percentages of training data, the performance of all three algorithms was comparable. With more training data, both GPR and BLR performed better than LSR.

It is important to put in context the high variance in RMS prediction error across users. This variance indicates how RMS prediction error changes from subject to subject. The variance was comparable to the mean error and appeared to be

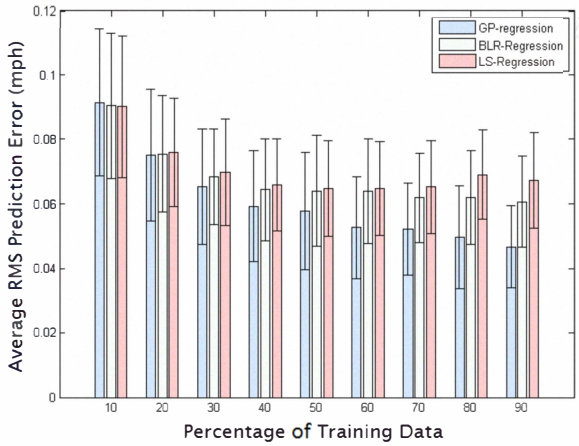

Figure 5: Relative performance of GPR, BLR and LSR on multiple subjects. Each bar shows average RMS error $\pm$ 1 standard deviation. Average RMS error across users decreases with relative increase of training data. GPR has a lower error than BLR or LSR. The variance across users is high indicating the diversity of the population.

independent of the algorithm used. These errors were averaged across a diverse range of subjects. The inherent diversity of the test subjects, while providing an adequate proof of concept for the algorithm contributed greatly to the variance of the prediction error. Walking speed has been shown to be a function of height, BMI, age and gender. The variances in prediction error were on the order of .1 mph. However, GPR had significantly lower RMS errors at 70%, 80%, and 90% training (all $p < 0.05$). Using large percentages of training data can still counter the effects of variance across users. Average error per user had a lower variance of .01 mph.

To provide a complete picture of algorithm performance, consider Fig. 7 which shows the average RMS prediction error for all three algorithms as a function of increasing training data in a single subject (subject 9). Data from subject 9 was chosen because of fine-grained speed information, though the results were equally valid on all other subjects. The variance was across multiple training instances with different randomly sampled training data and provided a measure of the repeatability of the speed-prediction capability. RMS prediction errors for both GPR and BLR decreased as a function of

Digital Object Identifier: 10.4108/ICST.PERVASIVEHEALTH2010.8786
http://dx.doi.org/10.4108/ICST.PERVASIVEHEALTH2010.8786

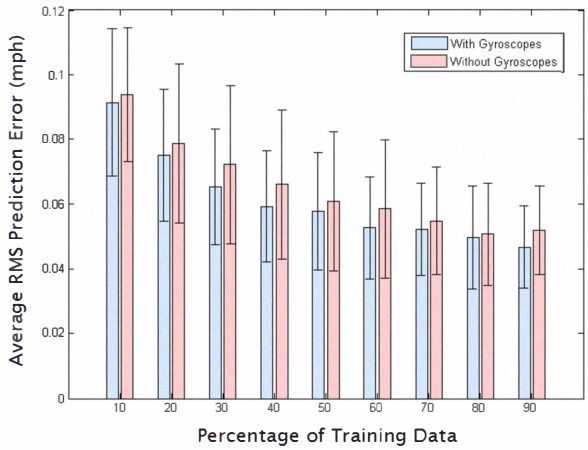

Figure 6: Effect of addition of gyroscopes across multiple subjects. Each bar shows average RMS error $\pm$ 1 standard deviation. Average RMS error is lower with addition of gyroscopes regardless of percentage of training data used.

increasing training data. GPR performed increasingly better than BLR under the same conditions. By contrast LSR showed much larger error with higher variance. This was expected as LSR is prone to overfitting and is not robust to outliers. Using ANOVA, the $p < 0.05$ at all training data percentages indicating that all results were statistically significant.
When data from each subject was analyzed individually, we saw that GPR showed a lower average RMS prediction error when compared with BLR and LSR. Even across subjects with a wide range of physical characteristics, GPR showed a significantly better performance when a larger relative percentage of training data was used. This indicates that GPR shows superior performance when a large quantity of data is available.

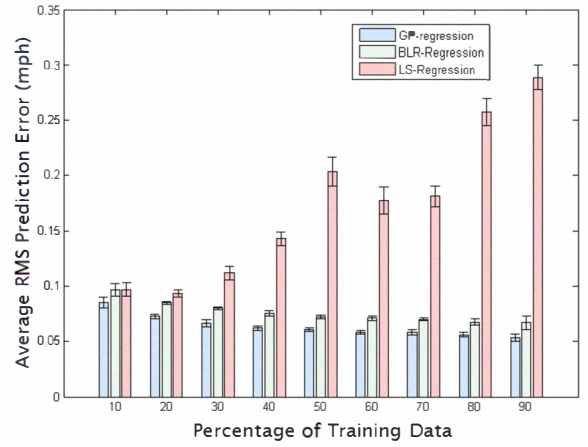

Figure 7: Relative performance of GPR, BLR and LSR on a single subject (subject 9).Each Bar shows average RMS error $\pm$ 1 standard deviation. Relative performance of GPR is far superior to LSR and better than BLR ($p>0.05$ in all cases). GPR has the least average RMS prediction error.

3) Effect of Window Size: The fundamental assumption in our approach is that the signal on which we train is periodic in nature. Each sliding window represents a time evolving snapshot of the signal. The FFT of this snapshot must capture this periodicity. This implies a minimum window size below which the periodicity is not sufficiently captured. Larger window sizes will provide increasingly finegrained information about the spectral components. However, the window cannot be made arbitrarily large as we have only a finite dataset. With this in mind, the choice of window sizes was narrowed down to 512 samples per window and 1024 samples per window. At 100 Hz sampling frequency, this approximately corresponds to a time window of 5 seconds and 10 seconds respectively. Fig. 8 illustrates the effect of using window sizes. Using a window size of 1024 resulted in a smaller RMS error ($p<0.05$ at 70% training and above). However, one can still use a window size of 512 if there is only a small training data set available.

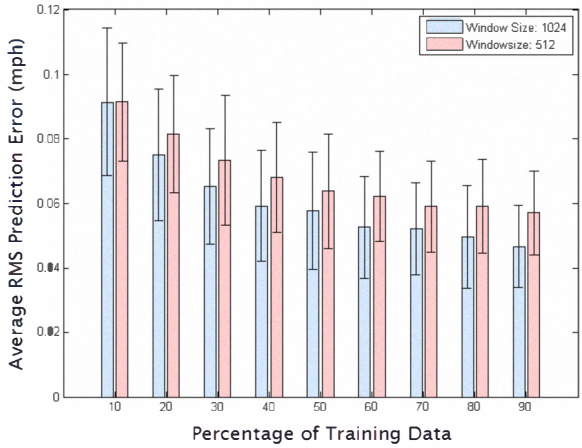

Figure 8: Comparison of window sizes of 1024 points per window ($\approx$10s) and 512 points per window ($\approx$5s) across multiple subjects. Each bar shows average RMS error $\pm$ 1 standard deviation. Average RMS error across users is less for 1024 points per window due to increased frequency resolution leading to fine-grained features being tracked.

4) Effect of Addition of Gyroscopes: The addition of gyroscopes provides information about torso rotational rates. Fig. 6 shows the average RMS prediction error across all users with and without gyroscopes for GPR. With increasing amount of training data, the difference in average RMS prediction error in the GPR case decreases. This suggests that one can offset the effect of not using gyroscopes with more training data. Using ANOVA, the p-values were greater than 0.05 in all cases, which must again be put in context considering variations across subjects. Per subject analysis shows that the addition of gyroscopes significantly reduces average RMS error ($p<0.05$ for all cases).

5) Per-Speed Accuracy: Fig. 9 shows the speed-wise RMS prediction error on test data (70% of data used for training, 1024 samples per window) on Subject 9. All speeds were uniformly sampled during the training phase. The prediction error was not uniform for all speeds. This leads to the interesting hypothesis that faster speeds constitute a different regime of walking. If so, there would be merit in separately training for these speed ranges thus offering the prospect of being able to separate out walking regimes. It must be remembered that our per-speed error results hold only for one subject and the same result might not generalize to other subjects. We aim to explore this in future work.

B. Predicting Overground Walking Speed

The second half of our experiments examined how treadmill data could be used in estimating overground walking speeds. It is easy to record samples and train models of movement data

Digital Object Identifier: 10.4108/ICST.PERVASIVEHEALTH2010.8786
http://dx.doi.org/10.4108/ICST.PERVASIVEHEALTH2010.8786

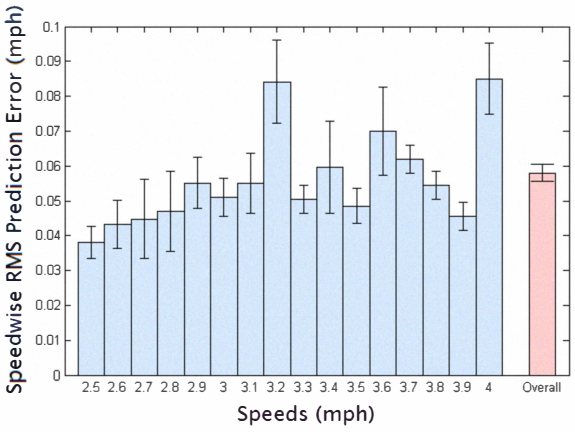

Figure 9: Per-speed accuracy as observed to subject 9. Accuracy is not uniform across speeds. Higher errors at higher speeds indicate a different walking regime.

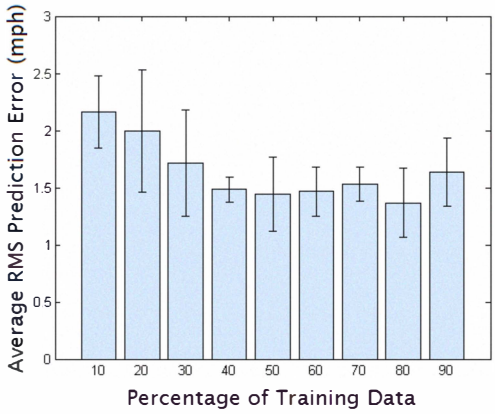

Figure 10: Increasing relative percentage of training data reduces the average RMS testing error. RMS errors are in the range of the speed themselves. This is due to consistent underestimation of GPR and the presence of a bias term.

for pre-determined speeds on a treadmill in closed laboratory settings. If this learned model could be used to predict overground walking speeds, it would present a scalable training method for obtaining personalized models. We focused on data collected from Subject 9. For each recording of overground walking, Subject 9 walked for a period of 11 seconds in a straight line on a flat, hard surface indoors. Treadmill data from subject 9 was used to train a GP model and speeds (in mph) were predicted for each overground walking dataset. Speeds were converted to appropriate units and multiplied by time travelled to give the predicted distance moved. Feature vectors were extracted (as explained in Sec. IV-C) using a window size of 1024 samples and using gyroscopic data.

1) Training and Testing on Overground Walking: We first trained and predicted from overground walking data alone. Fig. 10 shows our results. Training was done with GPR and average RMS testing error was calculated. Both the average error and variance did not decrease when more than 50% of the data was used for training. This was attributed to the small size of the original dataset due to which the algorithm would over-train and can be mitigated with larger sized recordings.

2) Using Treadmill Data to Predict Overground Walking Speeds: The second analysis addressed predicting overground walking speeds using only treadmill data for training. Fig.

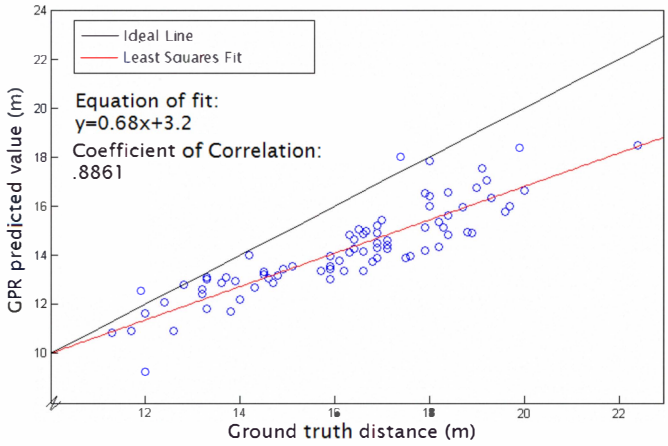

Figure 11: Line of best fit for prediction of overground walking in subject 9, shows high positive linear correlation.

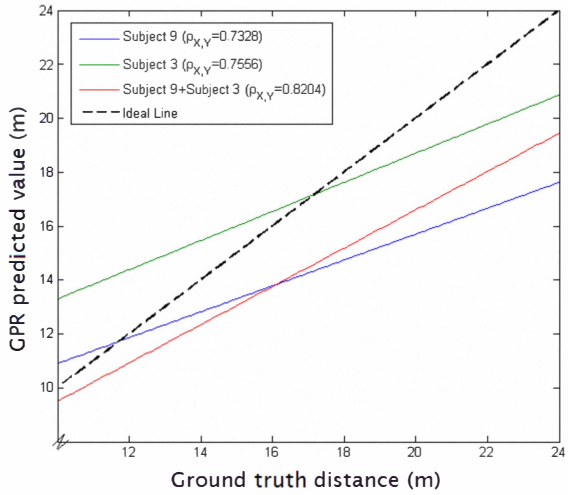

Figure 12: Combining data from two subjects with the same height significantly improves prediction of overground walking speed in one subject.

11 shows a scatter plot of GPR predicted values versus actual distance covered. We plot distance instead of speed as in our analysis, the two are related by $Distance = Speed\,(in\,mph) \times .44704 \times 11\,(m)$. The red-line indicates the line of best fit. The black line indicates the ideal line representing perfect correlation between ground truth and GPR predicted values. The slope tells us whether we overestimate or understimate the distance travelled. The y-intercept tells us how biased the treadmill dataset is for prediction. The slope and y-intercept of this line were 0.68 and 3.2 respectively. A value of 0.68 indicated that the distance was being underestimated. This was explained by the fact that in the beginning of each recording session, Subject 9 spent the first few seconds accelerating to a constant velocity, so the steady state walking assumption does not strictly hold. We tested for linearity with the Pearson's correlation coefficient defined as $r_{X,Y} = \frac{cov(X,Y)}{\sigma_X \sigma_Y}$. Analysis shows that $r_{X,Y} =$ .8861, indicating a high positive linear correlation ($p<0.05$).

3) Effect of Combining Treadmill Training Data from Multiple Subjects: We explored whether the use of data from people who share similar physical characteristics can significantly improve overground walking speed estimation on one of

Digital Object Identifier: 10.4108/ICST.PERVASIVEHEALTH2010.8786
http://dx.doi.org/10.4108/ICST.PERVASIVEHEALTH2010.8786

them. Data from Subject 3 (Height: 1.85 m, BMI 29) were chosen along with data from Subject 9 (Height: 1.82 m, BMI 21). Data from Subject 9 was downsampled by pruning out those speed recordings for which there was no analogous recording in Subject 3 thus forming the same equivalence class. Data from each subject were used separately as a source of training to predict distances covered by Subject 9. Data from both subjects were then combined into one training set as if from a "pseudo-subject" to predict the same distance. Fig. 12 shows the lines of best fit for each of the cases. An encouraging result was that although the equations of the lines of best fit for individual subjects (y=0.47x+7.9,$r_{X,Y} = 0.7328$ and y=0.54x+6.1,$r_{X,Y} = .7556$) were comparatively less accurate, the combined data showed a much better match (y=0.71x+2.4,$r_{X,Y} = .8204$). If generalizable this would mean that recording movement data for subjects with similar heights and grouping them together would enhance estimation accuracies. This would also facilitate practical data collection by encouraging small recordings on a large number of individuals. We aim to explore this further in future work.

VI. Conclusion

This paper described an application of Gaussian Process based Regression (GPR) in estimating walking speed from an on-body inertial sensor. GPR is a non-linear, non-parametric regression method. The frequency characteristics of signals from a tri-axial accelerometer and a tri-axial gyroscope were used to train a data-driven regression model. We compared the efficacy of GPR with well-known parametric techniques Least Squares Regression (LSR) and Bayesian Linear Regression (BLR).

Our results showed that GPR had a lower average RMS prediction error when compared to BLR and LSR across all subjects. Beyond 50% training data used, additional training data yielded small reductions in RMS error. Analysis on a single subject (Subject 9) showed that GPR had significantly lower RMS prediction error than LSR and BLR ($p<0.05$). Increase in relative percentage of training data in one subject greatly improved estimation of accuracy of both GPR and BLR with LSR displaying effects of over-fitting. Using a window size of 1024 samples resulted in a lower error across users as compared to using a window size of 512 samples because of an increased resolution in frequency features. The addition of tri-axial gyroscopes reduced the RMS prediction error of walking speeds when compared to using only acclerometers. The effect of introducing gyroscopes could be offset by using more training data. Prediction across all speeds on awas not uniform. Using GPR to estimate overground walking speeds from overground motion data alone resulted in reduced error with increase in relative percentage of training data. A strong linear correlation existed ($r_{X,Y} = .8861$) between overground walking speeds predicted from treadmill data and ground truth walking speed measured. Combining treadmill data from multiple subjects with similar height characteristics improved the prediction capability of GPR for overground walking speeds as measured by correllation between ground truth and GP-predicted values ($r_{X,Y} = .8204$ when data from two users was combined).

One limitation of our work is the generalizability of our approach across multiple subjects due to a large inter-subject variance. We plan to address this issue by performing a study on the prediction of treadmill walking speeds for a much larger population while labelling individual models in terms of physiological parameters such as age, height, gender and BMI. We aim to explore whether each of these models can be organized as clusters, each of which is a function of these parameters. The use of clusters would facilitate data collection by grouping people with similar physiological parameters in the same equivalence class. Using clusters might also enable extrapolation to new subjects who do not fall in a particular category. Finally we plan to explore the use of our techniques to map feature vectors directly to a measurement of energy expenditure. If successful, this will involve learning a data-driven functional mapping from the periodicity of walking to energy expended thus bypassing walking speed estimation.

Acknowledgements

This work was supported in part by Qualcomm, Nokia, NSF (CCR-0120778) as part of the Center for Embedded Network Sensing (CENS), and the USC Comprehensive NCMHD Research Center of Excellence (P60 MD 002254). Support for H. Vathsangam was provided by the USC Annenberg Doctoral fellowship program.

References

[1] S. T. Stewart, D. M. Cutler, and A. B. Rosen, "Forecasting the effects of obesity and smoking on u.s. life expectancy," *N Engl J Med*, vol. 361, no. 23, pp. 2252–2260, 2009.

[2] J. O. Hill, H. R. Wyatt, G. W. Reed, and J. C. Peters, "Obesity and the environment: Where do we go from here?," *Science*, vol. 299, no. 5608, pp. 853–855, 2003.

[3] A. L. Dunn, B. H. Marcus, J. B. Kampert, M. E. Garcia, H. W. Kohl III, and S. N. Blair, "Comparison of lifestyle and structured interventions to increase physical activity and cardiorespiratory fitness: A randomized trial," *JAMA*, vol. 281, no. 4, pp. 327–334, 1999.

[4] B. Ainsworth, W. Haskell, A. Leon, D. Jacobs, H. Montoye, J. Sallis, and R. Paffenbarger, "Compendium of physical activities: classification of energy costs of human physical activities.," *Medicine & Science in Sports & Exercise*, vol. 25, pp. 71–80, 1993.

[5] D. Spruijt-Metz, , M. Jerrett, J. Byrne, S. Hsieh, B. Xie, L. Wang, C.-P. Chou, and L. Reynolds, "Development, reliability and validity of an urban trail use survey.," *American Journal of Health Promotion*.

[6] K. Aminian and B. Najafi, "Capturing human motion using body-fixed sensors: outdoor measurement and clinical applications," *Computer Animation and Virtual Worlds*, vol. 15, no. 2, pp. 79–94, 2004.

[7] H. Luinge and P. Veltink, "Measuring orientation of human body segments using miniature gyroscopes and accelerometers," *Medical & Biological Engg & Computing*, vol. 43, no. 2, pp. 273–282, 2005.

[8] P. Esser, H. Dawes, J. Collett, and K. Howells, "Imu: Inertial sensing of vertical com movement," *Journal of Biomechanics*, vol. 42, no. 10, pp. 1578 – 1581, 2009.

[9] M. Rothney, M. Neumann, A. Beziat, and K. Chen, "An artificial neural network model of energy expenditure using nonintegrated acceleration signals," *J Appl Physiol*, vol. 103, pp. 1419–27, October 2007.

[10] S. Su, L. Wang, B. Celler, E. Ambikairajah, and A. Savkin, "Estimation of walking energy expenditure by using support vector regression," in *EMBS*, pp. 3526–3529, 2005.

[11] Y. Schutz, S. Weinsier, P. Terrier, and D. Durrer, "A new accelerometric method to assess the daily walking practice," *International Journal of Obesity*, vol. 26, pp. 111–118, January 2002.

[12] R. Herren, A. Sparti, K. Aminian, and Y. Schutz, "The prediction of speed & incline in outdoor running in humans using accelerometry," *Medicine and Science in Sports and Exercise*, vol. 31, no. 7, pp. 1053–1059, 99.

[13] J.-C. Cheng and J. M. F. Moura, "Tracking human walking in dynamic scenes," in *ICIP '97: Proceedings of the 1997 International Conference on Image Processing (ICIP '97) 3-Volume Set-Volume 1*, (Washington, DC, USA), p. 137, IEEE Computer Society, 1997.

[14] A. V. Rowlands, "Accelerometer assessment of physical activity in children: an update.," *Pediatr Exerc Sci*, vol. 19, pp. 252–266, Aug 2007.

[15] B. Zappa, G. Legnani, A. J. van den Bogert, and R. Adamini, "On the number and placement of accelerometers for angular velocity and acceleration determination," 2001.

[16] J. Widrick, A. Ward, C. Ebbeling, E. Clemente, and J. M. Rippe, "Treadmill validation of an over-ground walking test to predict peak oxygen consumption.," *Eur J Appl Physiol Occup Physiol*, vol. 64, no. 4, pp. 304–308, 1992.

[17] A. Branzan Albu, R. Bergevin, and S. Quirion, "Generic temporal segmentation of cyclic human motion," vol. 41, pp. 6–21, January 2008.

[18] C. Chang, R. Ansari, and A. Khokhar, "Efficient tracking of cyclic human motion by component motion," pp. 941–944, December 2004.

[19] C. E. Rasmussen and C. K. I. Williams, "Gaussian processes for machine learning (adaptive computation and machine learning)," 2005.

[20] C. K. I. Williams, "Prediction with gaussian processes: From linear regression to linear prediction and beyond," pp. 599–621, 1997.

[21] *IMU 6 Degrees of Freedom v4 Data Sheet - Sparkfun Electronics*.

Digital Object Identifier: 10.4108/ICST.PERVASIVEHEALTH2010.8786
http://dx.doi.org/10.4108/ICST.PERVASIVEHEALTH2010.8786